SWIMMERS' COLLECTIVE DYNAMICS MODELIZATION

Guillem Ferré
Supervisor: Ignacio Pagonabarraga

Abstract

We describe a new model in order to study the properties of collections of self-propelled particles swimming in a two-dimensional fluid. Our model consist in two types of particles, the first interacting with each other with a soft potential and thus representing the fluid while the second type are self-propelled particles of biological nature capable of changing its orientation following the velocity field of the fluid. The results of the simulations show how a super-diffusive regime arises at large times for biological particles, in addition to having higher velocity correlation. Also, it is show how the biological particles have a tendency to form clusters and how these particles tend to look for the same orientation.

1 Introduction

Our world is filled with microorganisms, and a great number of them are self-propelled microorganisms swimming in a fluid. Each of these microorganisms has its unique properties and propulsion method [1]. The physics of this swimming at micrometer scale are different from their counterpart at macroscopic scale, since at microscopic scale the viscosity is more important than inertia (leading us to low Reynolds number). In physics, this is translated into many particles systems that are out of equilibrium but that, like equilibrium systems in a phase transition, exhibit a cooperative behaviour.

Recently, many models entirely composed by orientated particles have been proposed in order to study collective properties. For instance, in the Vicsek model [2] the particles assume the average direction of the particles in their neighborhood with some noise, while their move at a constant module velocity. This simple model leads to a kinetic phase transition from no transport to finite net transport, that arises from a collective behaviour. Others models, such as the one made by Ginelli *et al.* [3], characterize by describing the particles with a complex position. This model also shows different phases, differentiated by the nematic order. Despite being simple, these models provide interesting results about the collective motion of swimmers, which is a matter of growing interest since recent works of mechanical systems driven by microorganisms [4].

2 The model

The motivation for our model is to couple the swimmers with a solvent and make sure that we recover the hydrodynamics. It arises from a new approach: As we want to modelize the dynamics of microorganisms swimming in a two-dimensional fluid, we consider two types of particles. The first type of particles are set up in order to represent a mesoscopic fluid system. These particles interact with each other and are governed by Newton's equations of motion.

$$\frac{\mathrm{d}\vec{r}_i}{\mathrm{d}t} = \vec{v}_i \,, m_i \frac{\mathrm{d}\vec{v}_i}{\mathrm{d}t} = \vec{f}_i \tag{1}$$

$$\vec{f}_i = \sum_{j \neq i} \left(\vec{F}^C_{ij} + \vec{F}^D_{ij} + \vec{F}^R_{ij} \right) \tag{2}$$

The sum is over all the particles found within a certain cutoff radius r_c from the particle i. The force that one particle experiences contains three parts: The first one, $\vec{F}^C_{ij}$, is a conservative force that particle j exerts on i, while the the second and third force are frictional and stochastic force, respectively.

Focusing on the conservative force, we choose it to be a soft repulsion that goes to zero by distances larger than r_c.

$$\vec{F}^C_{ij} = \begin{cases} a_{ij} \frac{r_c - r_{ij}}{r_c^2} \hat{r}_{ij} & r_{ij} < r_c \\ 0 & r_{ij} \geq r_c \end{cases} \tag{3}$$

In the equation above, a_{ij} is the maximum repulsion between particle i and j. Further information about this can be found at the paper by Groot and Warren [5].

In order to solve Newton's equations of motion, we use the velocity Verlet algorithm to find the position and velocities of the particles at time $t +$

Δt:

$$\vec{r}_i(t+\Delta t) = \vec{r}_i(t) + \Delta t \vec{v}_i(t) + \frac{\Delta t^2}{2m_i}\vec{F}_i^C(t) \tag{4}$$

$$\vec{v}_i(t+\Delta t) = \vec{v}_i(t) + \frac{\Delta t}{2m_i}\left(\vec{F}_i^C(t) + \vec{F}_i^C(t+\Delta t)\right)$$

In the equation above, $\vec{F}_i^C$ is the sum of the conservative forces acting on particle i. Following the paper by Lowe [6], we incorporate the other forces mentioned at 2 by implementing a thermostat. We construct a list of all pairs of particles for which $r_{ij} < r_c$. For each pair we decide, with a probability $\Gamma\Delta t$, whether to thermalize or not. The factor Γ is expected to correspond to the magnitude of the dissipative force. In order to thermalize, we generate a new relative velocity $[\vec{v}_{ij}]' \cdot \hat{r}_{ij}$ from a distribution $\xi_{ij}\sqrt{2k_BT/m}$, where ξ_{ij} is a Gaussian-distributed random variable with unit variance. To impose this new relative velocity on the pair of particles and conserve momentum, the new velocities are $[\vec{v}_i]' = \vec{v}_i + \vec{\Delta}_{ij}$ and $[\vec{v}_j]' = \vec{v}_j - \vec{\Delta}_{ij}$, where $2\vec{\Delta}_{ij} = \hat{r}_{ij}([\vec{v}_{ij}]' - \vec{v}_{ij}) \cdot \hat{r}_{ij}$.

Once the particles representing the fluid mesoscopically are implemented, it's time to add the active particles that represent the swimmers. The dynamics of these active particles also follow Newton's equations of motion 1, and use the same integrator as the fluid particles (or passive particles) 4. Since we have a new set of particles, three interactions between particles now exist: a) Interaction between passive particles, b) interaction between active particles and c) interaction between an active and a passive particles. In the three cases, the interaction follow the same conservative force (equation 3), but the maximum repulsion a_ij changes. First, we will say that the maximum repulsion doesn't depend on the particles i and j. Second, we distinguish between two maximum repulsion values: a_1 and a_2, being the first one for interactions a) and c), and the second one for interactions of type b). Finally, in this work we will use $a_2 = 0$, which means that active particles doesn't interact between them. This is meant to facilitate the formation of clusters. Also, the active particles present a orientation $\hat{n}_i$ and they are self-propelled with a constant velocity v_0 in this direction. In the velocity Verlet integrator, this is reflected with a new term $\hat{n}_i \cdot v_0$ in the position update, that must be modified in order to conserve the momentum of the system. For the thermostat this propulsion velocity isn't taken into account since the thermalization is done with the "thermal" velocity only, which is the velocity of the particles of the thermal bath. This v_0 term in the velocity will cause a lift in the temperature from the expected value without propulsion.

Our model also allow the active particles to rotate following the fluid flow, so the rotation of the particle must depend on the velocities of all particles around it. A particle i rotation during a time interval Δt can be expressed as $\Delta\theta_i = \omega_i\Delta t$, where ω_i is the vorticity sensed by the particle. At a given time step, one can compute the angular momentum $\vec{L}_i = \sum_{j\neq i}\vec{r}_{ij} \times \vec{v}_j$ of the particle i. In order to find the vorticity in terms of the velocities of the particles, we approximate $\vec{v}_j \simeq \bar{v}_i + r_{ij\alpha}\nabla_\alpha\vec{v}_\beta$, where $\bar{v}_i = \sum_{j\neq i}\vec{v}_j$. We choose $\vec{v}_j$ in this way, as a first term expansion around a constant value $\bar{v}_i$, since then each velocity belonging to a particle j will have a dependence in the vorticity of particle i. Is important to note that, despite the rotation being only computed for the active particles, the velocity of all the particles (active and passive) within r_c are counted in order to compute the vorticity.

With the approximation mentioned above, we find $\vec{L}_i = \sum_{j\neq i}(\epsilon_{\alpha\beta\mu}\vec{r}_{ij\beta}\vec{r}_{ij\delta}(\nabla_\delta\vec{v}_\mu) + \vec{r}_{ij} \times \bar{v}_i)$. Since $\sum_{j\neq i}\vec{r}_{ij\beta}\vec{r}_{ij\delta}$ can be written as $\delta_{\beta\delta}\frac{1}{2}\sum_{j\neq i}r_{ij}^2$, then $\epsilon_{\alpha\beta\mu}\delta_{\beta\delta}\nabla_\delta\vec{v}_\mu = \epsilon_{\alpha\delta\mu}\nabla_\delta\vec{v}_\mu = \nabla \times \vec{v}$. Isolating $\nabla \times \vec{v} = \vec{\omega_i}$, we finally obtain the vorticity in order to compute the rotation of the active particles at each time step:

$$\vec{\omega_i} = \sum_{j\neq i}\vec{r}_{ij} \times (\vec{v}_j - \bar{v}_i)\frac{2}{\sum_{k\neq i}r_{ik}^2} \tag{5}$$

Since with the rotation we change the velocity of the particle i, in order to conserve the momentum we must subtract a fraction $1/N$ of the velocity change of particle i to all the particles within r_c, where N is the number of particles within that range. This way, the total momentum is conserved, and with a large number of total particles the variations to their velocity are small due to the factor $1/N$. In our model, the computation of the vorticity for all active particles is performed before the updating of positions, while the rotation of $\hat{n}_i$ occurs after updating positions and velocities. That means that the active particle flips following the velocity field existing in the time step before.

Since the soft potential of our conservative force doesn't cause a strong repulsion at short distances, in the initialization of the system the two types of particles are placed randomly in the cell. Also, the orientation of active particles are set randomly, same as the velocity of all particles. Then we proceed to setting the total momentum to zero and performing an scaling of velocities, without the propulsion term like in the thermostat, in order of have the thermal bath velocities. In order to conserve the momentum and mass of the system, and to avoid problems with the borders of the box, our model use periodic boundary conditions and the simulation is run in a box with side L.

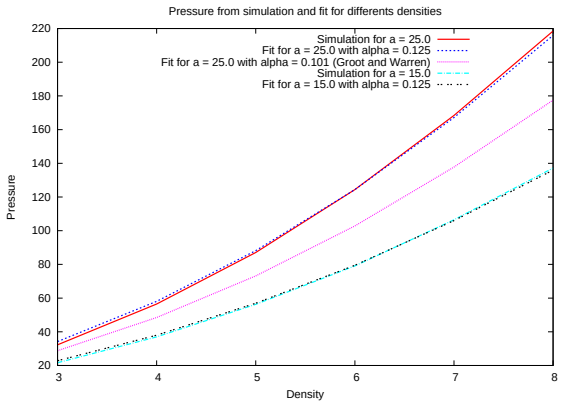

Figure 1: Pressure computed (in red) for densities ranging from 3.0 to 8.0, for values of $a = 25.0$ and $a = 15.0$. Fit for different values of α, being $\alpha = 0.125$ the one fitted with our data and $\alpha = 0.101$ the one given by Groot and Warren.

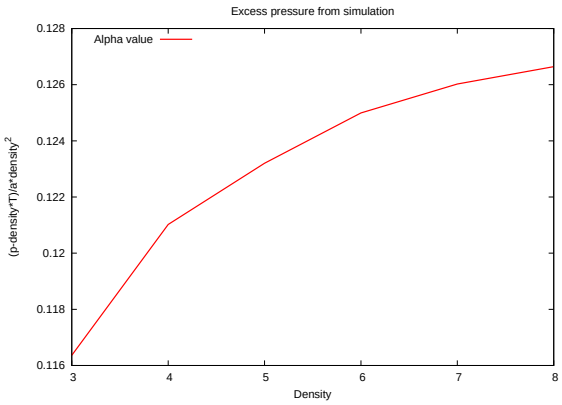

Figure 2: Excess pressure divided by $a\rho^2$, case with $a = 25.0$. Larger densities are needed in order to find reach a constant value of α.

3 Testing the model

In order to test that our program has the model implemented correctly, we perform a series of simulations to verify it. Hence, we set the parameters of the simulation towards having only passive particles, thus representing only the fluid. We choose of $r_c = 1.0$ and $m = 1$, since we will be working with box sizes $L \sim 10$. Maximum repulsion is chosen as $a_1 = 25$, $\Delta t = 0.001$ and a thermal velocity of $v_t = 2.0$ which means a temperature of the bath equal to $T = 2.0$. With this parameters and the thermostat always active we can compute different properties of the simulated fluid in order to verify the correct performance of the model.

First of all, one can obtain the internal pressure of the system by using the virial theorem. Following this, the pressure can be computed as follows:

$$p = \rho k_B T + \frac{1}{dV} \sum_{j>i} \vec{r}_{ij} \cdot \vec{F}_{ij}^{C} \qquad (6)$$

where, since we are working in a two-dimension, $d = 2$ and the volume is $V = L^2$. The first term of the expression is easily computed while the second one is a little more costly and unpredictable. While working in three dimension, Groot and Warren [5] provide a good approximation for the pressure that holds for sufficiently high densities ($\rho > 2$):

$$p = \rho k_B T + \alpha a \rho^2 \qquad (7)$$

where a is the maximum repulsion of the particles and α is a fit parameter that they calculated as being $\alpha = 0.101 \pm 0.001$. We perform a simulation using $a = 25.0$ as Groot and Warren and compute our value of α.

As shown in figure 1 it can be seen how the behaviour of our pressure, both for $a = 15.0$ and $a = 25.0$, follows clearly a parabola with $\alpha = 0.125 \pm 0.001$. In the figure the parabola with $\alpha = 0.101$ is also shown in order to compare differences. As can be seen, our values of pressure for $a = 25.0$ are higher than the ones obtained by Groot and Warren, hence some sort of difference between the two models must exist. As we said before, seems plausible to think that the differences come from the dimensions of the simulation, although we haven't check it. Since the proportionality of the pressure to ρ^2 came from the second term of the equation 6, one can compute the excess pressure as $p - \rho k_B T$ and divide it by $a\rho^2$ in order to see how fast α tends towards a constant value. In figure 2 one can see how α value for these densities doesn't reach a constant value, while Groot and Warren [5] achieve this with values of density $\rho \sim 4$. Since we are working in a two-dimensional system some differences with the results can be expected, and ours behave correctly enough.

One can also compute the correlation function $g(r)$ in order to see if the behaviour is the one expected also by Groot and Warren. As before, we use $a = 25.0$ and a density of $\rho = 3$. The results are shown in figure 3, and one can see how the shape of the distribution function is the one expected from a soft potential.

With this results we prove that our program works correctly while only having fluid particles. When we add the self-propelled particles, we expect a few changes from this results. First, the temperature T of the system will be different (higher) from the one from the bath T_{bath}, since the propulsion velocity add a factor unseen by the thermostat. In order to see this, we compute the kinetic energy for active and passive particles and

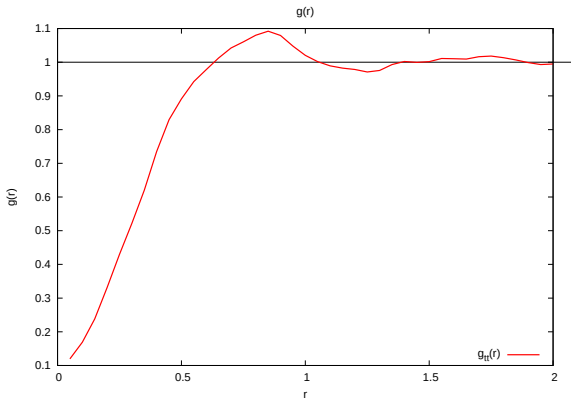

Figure 3: Distribution function $g(r)$ for our soft potential for $\rho = 3$ and $a = 25$

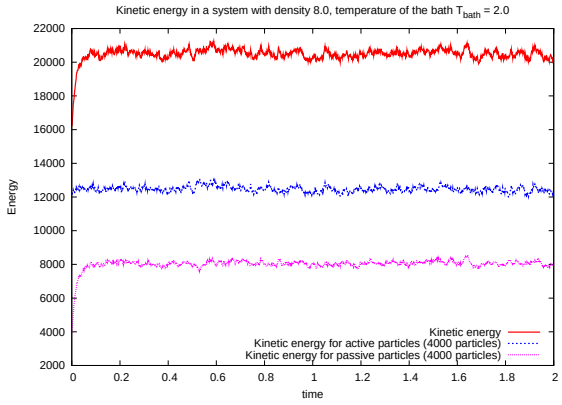

Figure 4: Time series of kinetic energy for active and passive particles, and total. The mean values, once thermalized, are $K_{active} = 12469 \pm 4$, $K_{passive} = 8020 \pm 7$ and $K_{total} = 20489 \pm 8$. The mean temperature of the system is $T = 2.561 \pm 0.001$

the temperature of the system at each time step, then compute the mean value of all the time series. In this simulation we use $a_1 = 5.0$, $\Delta t = 0.001$ with a total number of steps of $N_{steps} = 2000$, a density of $\rho = 8.0$ and 4000 particles of each type. The thermal velocity is set at $v_t = 2.0$ as before, thus having a temperature $T_{bath} = 2.0$, and the propulsion velocity is set a $v_0 = 1.5$. As shown in the figure 4, the time series shows a fast thermalization after which the temperature of the system remains quite constant. From the kinetic energies one can obtain the temperatures of both type of particles: Passive particles are a temperature $T_{passive} = 2.005$, that of the thermal bath, while active particles $T_{active} = 3.117$. This cause the total temperature of the system to be $T = 2.561$, as computed directly from the times series of the temperature. One can note how the temperature of the active particles is different from $v_t + v_0$, since the orientation of $\vec{v}_i$ and $v_0 \cdot \vec{n}_i$ are different.

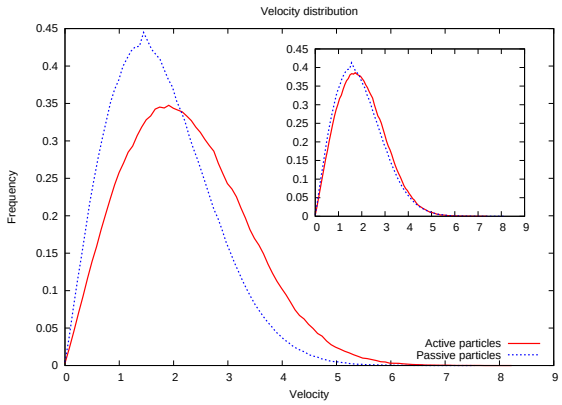

Figure 5: Velocity distributions for a system with $\rho = 8.0$, $a_1 = 5.0$, $v_0 = 1.5$, $v_t = 2.0$, with a density of active particles $n_{active}/n_{total} = 0.375$. At the small windows we have typified the graphs.

4 Results

Here we are going to discuss some properties about the swimming particles that we observed with this model. First we made a brief study about the velocities of the particles, active and passive. The velocity distributions for both types of particles can be observed at figure 5, where active particles have a wider distribution since propulsion velocity is added to the typical thermal velocity of the particle. At the small graph at 5 we have typified both graphs thus we can see how both almost coincide at the same Gaussian. From just looking one can say that the mean velocity of these Gaussians is $v_{mean} \sim 2.0$, which agree with $v_t = 2.0$ we are using in this simulation. One can also look at velocity correlation (figure 6) in order to note some differences. There we see how passive particles at long time scales have a slope ~ -1, an algebraic decay $1/t$ which is the long time tail of the hydrodynamics. On the other hand, active particles have a higher correlation. It would be interesting to see if at larger times active particles also decay algebraically as $1/t$. This is an open question left to be understood. One can expect this correlation to became higher if we increase the value of propulsion velocity v_0.

One can also look for the mean square displacement of particles since, as velocity correlation, can give information about the diffusion. At figure 7 one can see it for both active and passive particles. There we can see how until $t \sim 0.1$ both active and passive particles have a ballistic behaviour since MSD increases as t^2. However, it can be seen that

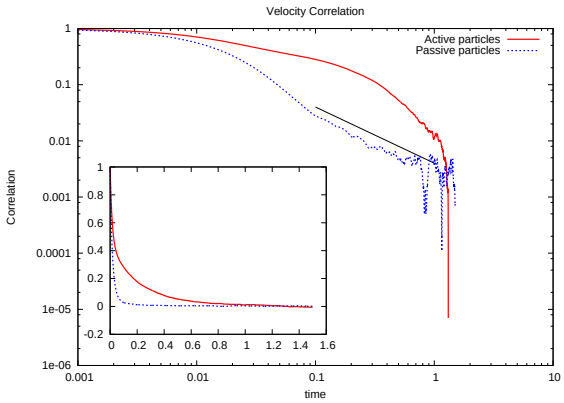

Figure 6: Velocity correlation in logarithmic scale for a system with $\rho = 8.0$, $a_1 = 5.0$, $v_0 = 1.5$, $v_t = 2.0$, with a density of active particles $n_{active}/n_{total} = 0.375$. At the small windows the correlation is plotted without logarithmic scale.

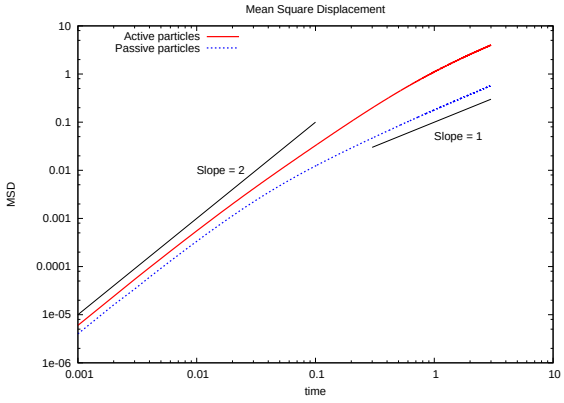

Figure 7: Mean square displacement in logarithmic scale for a system with $\rho = 8.0$, $a_1 = 5.0$, $v_0 = 1.5$, $v_t = 2.0$, with a density of active particles $n_{active}/n_{total} = 0.375$.

passive particles leave ballistic behaviour before active particles do, and thus reach diffusive behaviour (t^1) before, too. The values of mean square displacement are higher for active particles since they have the propulsion velocity, so one can expect the values to increase further for larger values of v_0. Also, it seems that near $t \sim 1$ passive particles began to reach the diffusive behaviour. For active particles there is an intermediate super-diffusive regime before reaching a diffusive behaviour, with a crossover time between the two regimes. In further analysis it could be interesting to see how this crossover time increases with the activity.

Now our objective is to look for a collective behaviour in the active particles. In order to do so we compute the distribution function $g(r)$ for all particles and ones for only active or passive particles. The results are shown in the figure 8. One can see how the distribution function for all particles g_{tt} is similar to the one expected for a fluid, although it doesn't go to zero at distances $r \sim 0$. For the distribution only for passive particles, g_{pp}, we see how it follows g_{tt} quite closely and shows a behaviour similar to the one at 3, so the passive particles doesn't present any important change between a system with active or without active particles. For g_{ap} we can see how more of passive particles stand at $r > r_c$ from active particles. On the other hand, g_{aa} shows that active particles form clusters since they have a high concentration at $r \sim r_c/2$. It also present a minimum at $r \sim r_c$. This attractive behaviour observed despite active particles don't attract each other arises from the repulsion a_1 of passive particles, that cause active particles to form this clusters. When computing cluster sizes later, we will choose $r_c/2$ as the maximum distance two particles can have from each other in order to form a cluster.

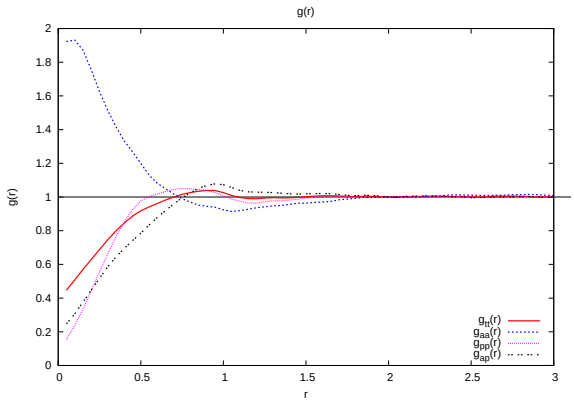

Figure 8: Distribution functions for a system with density $\rho = 4.0$, $a_1 = 25.0$, $v_0 = 1.5$, $v_t = 2.0$, with a density of active particles $n_{active}/n_{total} = 0.375$

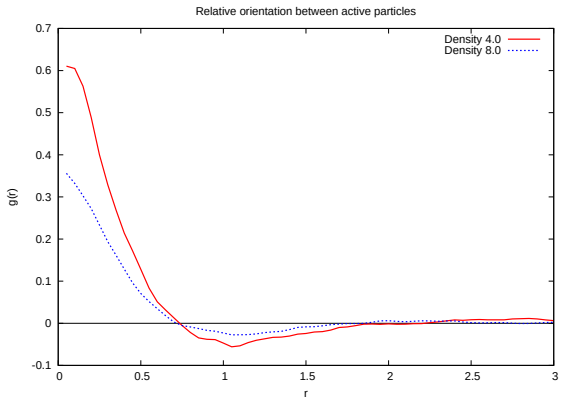

Figure 9: Relative orientation between active particles for $a_1 = 25.0$, $v_0 = 1.5$, $v_t = 2.0$, with a density of active particles $n_{active}/n_{total} = 0.375$

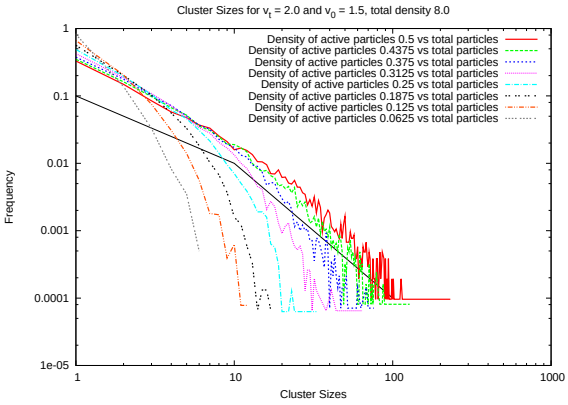

Figure 10: Cluster distributions for different values of active particles' density n_{active}/n_{total}, in a system with $\rho = 8.0$, $a_1 = 5.0$, $v_0 = 1.5$, $v_t = 2.0$. A line is plotted with slope -1 and -2 in order to ease comparisons.

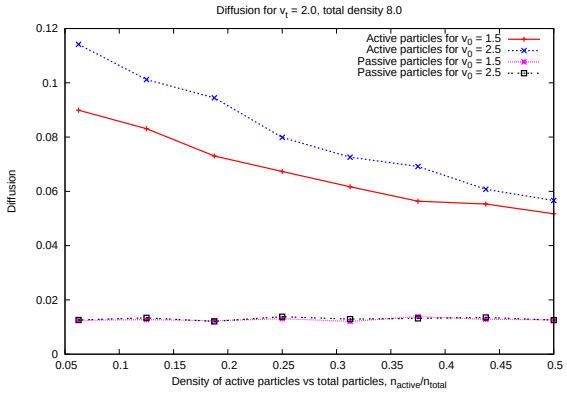

Figure 11: Diffusion of both active and passive particles in function of density of active particles n_{active}/n_{total} in a system with $\rho = 8.0$, $a_1 = 5.0$, $v_t = 2.0$ and for both $v_0 = 1.5$ and $v_0 = 2.5$.

Also, we want to see if close active particles tend to align his vectors $\vec{n}$ in the same direction. In order to do so, we compute a distribution function weighed as $|cos\theta|$. Since generally the orientation of $\vec{n}$ is equiprobable, we need to subtract $2/\pi$ since we are working with absolute value of $cos\theta$. This is shown at figure 9 for two different total densities, $\rho = 4.0$ and $\rho = 8.0$. There we can see how, at distances $r > 2.0$ the orientation tends to zero, meaning that no relation exist between two particles to orient in the same direction. At small distances $r < 0.5$, however, we can see how a relative orientation arises. At average, active particles closely enough tend to have an orientation of $\cos\theta \sim 0.6$ for density $\rho = 4.0$ and $\cos\theta \sim 0.35$ for density $\rho = 8.0$, thus particles are closely aligned for low densities. Despite these are not phases of totally aligned particles inside a cluster, the results clearly differentiate between randomly relative orientation and a clear relative alignment.

Now we can compute the cluster sizes that form the active particles and see how they change for different densities of active particles n_{active}/n_{total}. As we said before, we choose two particles to be in the same cluster if the distance between them is lower than $r_{ij} < r_c/2$, since most of the active particles found more active particles inside this radius (figure 8. At figure 10 one can see the clusters' distributions for a system with a fixed density $\rho = 8.0$, but for different number of active particles. We see how with a low density of active particles the clusters formed are very small and the maximum number of particles is ~ 10. As density rises one can see how the distribution became wider and clusters with sizes ~ 100 can be observed when the number of active particles is near the half of total particles. At this state, $n_{active}/n_{total} = 0.5$, we can see how the cluster distribution has two slopes. Until cluster sizes of 10 the slope follows almost -1, while past this number the distribution falls as ~ -2. In the process of forming cluster, incrementing the propulsion velocity doesn't has any consequence in the distributions, incrementing nor decreasing the slopes. It's important to note that the tendecies of the clusters' distribution doesn't vary if we change the criteria for which two particles belong to the same cluster. So if we say that two particles belong to the same cluster if the distance between them is lower than $r_c/4$ the number of clusters will increase but the tendecy of the distribution would be the same.

Finally, we compute the diffusion of active and passive particles when the ratio of active particles over the total number of particles varies, as shown in figure 11, for two different values of propulsion velocity v_0. There we can see how, despite the total density of the system being constant for all the points, the diffusion varies with the density of active particles. Passive particles' diffusion remains almost constant for all values and for both $v_0 = 1.5$ and $v_0 = 2.5$, as is expected since the fluid's diffusion shouldn't change as long as the total density of the system remains the same. For active particles we see how the diffusion rise as we lower the number of active particles in the system. Since repulsion between passive particles create a fictional attractive force between active particles, decreasing its number cause less clusters to be formed. Also, this behaviour of having an increasing diffusion as fraction of active particles decreases is similar to the one observed for gases, where when the density of the system decreases the diffusion rises since more free space is available. This reflects that, despite share the space with passive particles, active particles' diffusion behaviour doesn't seems

to care at all for passive particles. Of course, the diffusion for active particles also increases with v_0.

5 Conclusions

With this work we have develop a new model that couples swimmers with a solvent so we can study further the collective properties of swimming microorganisms. We provide different results in order to assure that the hydrodynamics obtained are the expected, and to look at the properties of the swimming particles we inserted in the fluid.

We have seen how the velocity correlation gives the result one expects in a fluid for the passive particles, thus recovering the hydrodynamics result. Also one sees how the correlation is greater for active particles. As we noted before, in future works it would be interesting to see if at larger times the active particles achieve an algebraic decay $1/t$. Also, the mean square displacement for the passive particles behaves as expected for a fluid while the one for active particles presents an intermediate super-diffusive regime between ballistic and diffusive behaviours. In this work we only mention the existence of this regime, but a further analysis about how this crossover time varies with the activity would be interesting to study in future works.

The model also shows an inclination of the swimmers to form clusters, and we see how a tendency in the clusters' distribution arises when the density of active particles reach certain values. The swimmers also have a tendency to orientate themselves, while forming a cluster, in the same direction, although we haven't reach a state where all the particles in a cluster are totally parallel or antiparallel.

References

[1] E. Lauga and T. R. Powers, "The hydrodynamics of swimming microorganisms," *Reports on Progress in Physics*, vol. 72, no. 9, p. 096601, 2009.

[2] T. Vicsek, A. Czirók, E. Ben-Jacob, I. Cohen, and O. Shochet, "Novel type of phase transition in a system of self-driven particles," *Phys. Rev. Lett.*, vol. 75, pp. 1226–1229, Aug 1995.

[3] F. Ginelli, F. Peruani, M. Bär, and H. Chaté, "Large-scale collective properties of self-propelled rods," *Phys. Rev. Lett.*, vol. 104, p. 184502, May 2010.

[4] A. Sokolov, M. M. Apodaca, B. A. Grzybowski, and I. S. Aranson, "Swimming bacteria power microscopic gears," *PNAS*, vol. 107, pp. 969–974, January 2010.

[5] R. D. Groot and P. B. Warren, "Dissipative particle dynamics: Bridging the gap between atomistic and mesoscopic simulation," *J. Chem. Phys.*, vol. 107, pp. 4423–4435, Sept. 1997.

[6] C. P. Lowe, "An alternative approach to dissipative particle dynamics," *EPL (Europhysics Letters)*, vol. 47, no. 2, p. 145, 1999.